Transverse Velocity Scaling in Au+Au Midrapidity Emissions

J. Łukasik[6,10], G. Auger[1], Ch.O. Bacri[2], M.L. Begemann-Blaich[6], N. Bellaize[3], R. Bittiger[6], F. Bocage[3], B. Borderie[2], R. Bougault[3], B. Bouriquet[1], Ph. Buchet[4], J.L. Charvet[4], A. Chbihi[1], R. Dayras[4], D. Doré[4], D. Durand[3], J.D. Frankland[1], E. Galichet[5], D. Gourio[6], D. Guinet[5], S. Hudan[1], B. Hurst[3], H. Orth[6], P. Lautesse[5], F. Lavaud[2], J.L. Laville[1], C. Leduc[5], A. Le Fèvre [6], R. Legrain[4], O. Lopez[3], U. Lynen[6], W.F.J. Müller[6], L. Nalpas[4], E. Plagnol[2], E. Rosato[7], A. Saija[8], C. Sfienti[6], C. Schwarz[6], J.C. Steckmeyer[3], G. Tăbăcaru[1], B. Tamain[3], W. Trautmann[6], A. Trzciński[9], K. Turzó[6], E. Vient[3], M. Vigilante[7], C. Volant[4], B. Zwiegliński[9] and A.S. Botvina[6]
(The INDRA and ALADIN Collaborations)

[1] *GANIL, CEA et IN2P3- CNRS, B.P. 5027, F-14076 Caen, France,* [2] *Institut de Physique Nucléaire, IN2P3-CNRS et Université, F-91406 Orsay, France,* [3] *LPC, IN2P3- CNRS, ISMRA et Université, F-14050 Caen, France,* [4] *DAPNIA/SPhN, CEA/Saclay, F-91191 Gif sur Yvette, France,* [5] *Institut de Physique Nucléaire, IN2P3-CNRS et Université, F-69622 Villeurbanne, France,* [6] *Gesellschaft für Schwerionenforschung mbH, D-64291 Darmstadt, Germany,* [7] *Dipartimento di Scienze Fisiche e Sezione INFN, Univ. Federico II, I-80126 Napoli, Italy,* [8] *Dipartimento di Fisica dell' Università and INFN I-95129 Catania, Italy,* [9] *A. Sołtan Institute for Nuclear Studies, Pl-00681 Warsaw, Poland,* [10] *H. Niewodniczański Institute of Nuclear Physics, Pl-31342 Kraków, Poland*

Abstract. The emission of intermediate-mass fragments in collisions of ^{197}Au on ^{197}Au was systematically studied over the range of incident energies from 40 to 150 A MeV using the 4π-multidetector INDRA and beams from the heavy-ion synchrotron SIS at GSI Darmstadt. The analysis was performed as a function of incident energy and of impact parameter, defined through the total transverse energy of light charged particles (Etrans12, $Z \leq 2$). This observable was found to scale linearly with the collision energy up to a certain limit above which it saturates. Strong forward–backward asymmetries in the emission pattern with respect to the rapidities of the projectile and target residua were observed. Their possible relation to equilibration is discussed and interpreted in the framework of molecular dynamics and statistical multifragmentation models. Transverse velocities at midrapidity for peripheral collisions were found to show a surprisingly weak dependence on the incident energy. On the contrary, transverse velocities at midrapidity for central collisions showed a strong dependence on incident energy indicating an increasing importance of collective flow with increasing bombarding energy.

INTRODUCTION

Experimental data obtained during the 4^{th} INDRA Campaign carried out at GSI permit the study of the collisions of both symmetric (Au+Au, Xe+Sn) and asymmetric (C+Au, C+Sn) systems in a broad energy range. This energy range spans an interesting transition region from around the Fermi energy (40–50 A MeV) up to relativistic energies approaching the participant–spectator domain (150–250 A MeV) for symmetric systems, and a range of relativistic bombarding energies (95–1800 A MeV) for asymmetric ones.

Despite of the pronounced binary character of non-central symmetric heavy ion collisions, a sizable amount of detected particles and fragments have parallel velocities intermediate between those of the projectile and of the target [1–4] and their importance increases with increasing centrality of the collision. They are often referred to as *midrapidity* (*midvelocity*) emissions. These emissions seem to be strongly influenced by dynamical effects and are thought to proceed on a relatively short time scale. The associated reaction scenarios include fast pre-equilibrium particles, particles and fragments emitted from the neck, as well as light fission fragments preferentially aligned in

between the two main reaction partners. This leads to the question whether a description as statistical emission from a well–defined source, a generally very successful concept for multifragmentation, can be ruled out for the midrapidity component. We will concentrate on this point in the first part of this contribution, after having introduced the chosen centrality selection. In the second part, we will show that transverse velocities of fragments seem to be a particularly efficient source of information and discuss their scaling properties as a function of impact parameter and bombarding energy.

CENTRALITY SELECTOR

One of the properties of the INDRA detector [5] is its high efficiency (about 90%) for light charged particles (LCP, Z=1,2), independently of the type of the reaction mechanism involved and hence of the impact parameter. We therefore use in the following the total transverse energy, Etrans12, of LCP as an impact parameter selector.

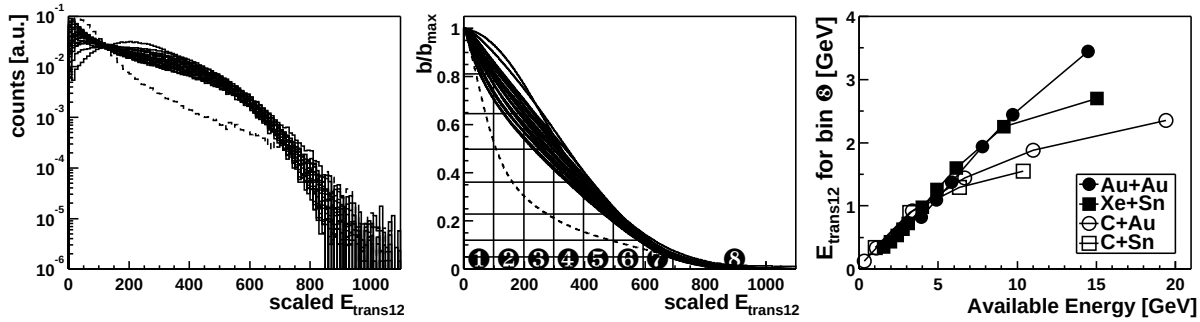

FIGURE 1. Left panel: scaled transverse energy spectra of Z$\leq$2 particles (Etrans12) for 23 systems studied during the 4^{th} INDRA Campaign: Au+Au @ 40, 50, 60, 80, 100, 150, Xe+Sn @ 50, 65, 80, 100, 150, 250, C+Au @ 30, 95, 300, 600, 1000, 1800, C+Sn @ 95, 300, 600, 1000 A MeV (solid lines) and C+U @ 1000 A MeV (dashed line); Middle panel: reduced impact parameter derived from the scaled spectra with the indicated binning of Etrans12 and b/b_{max} for Au+Au @ 60 A MeV. Right panel: Etrans12 for the most central collisions (bin ❽) versus the available CM energy of the systems specified above, except the C+U reaction. The first 4 points for the Xe+Sn reactions at 25, 32, 39 and 45 A MeV were taken from the 1^{st} INDRA Campaign [4].

The left panel of Fig. 1 presents distributions of scaled Etrans12 for 23 systems that were studied during the 4^{th} INDRA Campaign (see caption). Etrans12 of each system was scaled here to match the spectrum of Xe+Sn @ 50 A MeV. As can be seen, all the spectra have similar shapes, and by changing the Etrans12 scale they can be superimposed on top of each other for both symmetric and asymmetric systems. The only exception seems to be the reaction C+U @ 1000 A MeV, probably due to the large cross section for fission in this reaction.

The middle panel presents the relation between the scaled Etrans12 and the reduced impact parameter, b/b_{max}, obtained with the use of the geometrical prescription [6]. The last bin (bin ❽) corresponds to 5% of b_{max}. The remaining part of the Etrans12 spectrum was divided into 7 equal bins, with bin ❶ corresponding to the most peripheral collisions.

The right panel of Fig. 1 presents the relation between Etrans12 for bin ❽ and the total available energy in the center of mass (CM) frame of the Au+Au, Xe+Sn, C+Au and C+Sn systems. For symmetric systems, the spectra scale linearly with the available CM energy, up to about 100-150 A MeV (see also [4]). Above this threshold a saturation effect can be observed. For asymmetric systems the saturation is visible above 300 A MeV. This saturation can be partly related to the fact that at relativistic energies the nucleon-nucleon cross section becomes more forward peaked reducing the conversion of incident energy into transverse energy and leading to some transparency effects. On the other hand, instrumental effects may also play a role here. The increasing number of multihits and punch-through hits with increasing incident energy may lead to a higher probability for mis- or nonidentification or imperfect measurement of energy.

MIDRAPIDITY EMISSIONS: DYNAMICAL AND STATISTICAL SCENARIOS

A pronounced two source picture of peripheral collisions of symmetric heavy systems is always (even at highest, 150 A MeV energy) accompanied by an important contribution of midrapidity fragments. This can be inspected from the left panel of Fig. 2, which presents the invariant cross section plot of lithium ions from Au+Au reaction at 80 A MeV

for peripheral collisions (bin ❸). The included histogram represents the projection of this 2 dimensional distribution on the rapidity axis.

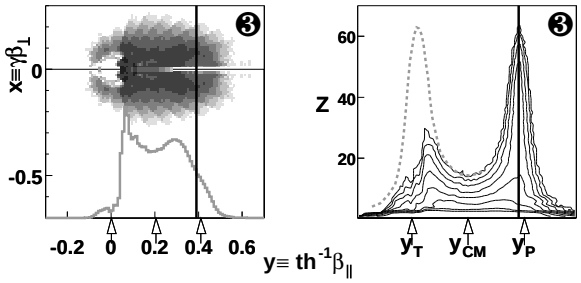

FIGURE 2. Left panel: invariant cross section plot of lithium ions from Au+Au reactions at 80 A MeV for peripheral collisions (bin ❸). The included histogram represents the projection on the rapidity axis. Right panel: contour plot of Z vs rapidity for fragments from the same reaction. The arrows denote the target, CM and projectile rapidities, respectively. The vertical line in both panels corresponds to the mean rapidity of heavy projectile-like fragments.

The right panel of Fig. 2 presents rapidity distributions of all fragments from the same reaction. The vertical lines correspond to the mean rapidity of heavy projectile-like fragments. It is drawn to emphasize the strong forward-backward asymmetry in the emission of lighter fragments. The dashed line is meant to indicate that, because of the symmetry of the system, the same pattern is expected in the target-side region where, however, thresholds limit the detection of heavy fragments. The arrows denote the target, CM and projectile rapidities, respectively. The figure clearly shows that intermediate mass fragments (IMFs, $3 \leq Z \leq 20$) are preferentially emitted towards midrapidity, in between the rapidities of the heavy target and projectile residua.

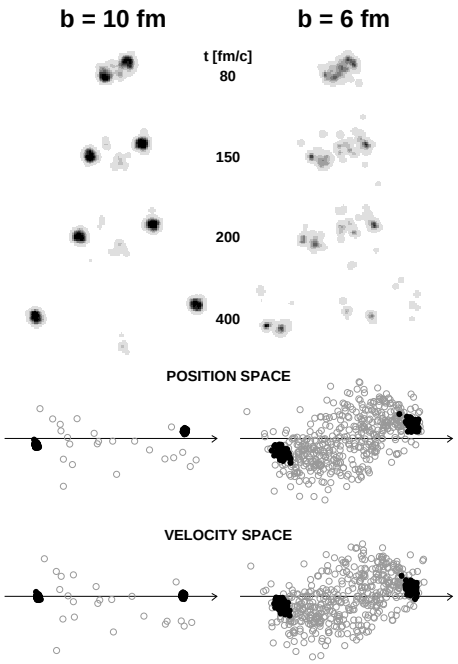

FIGURE 3. CHIMERA predictions for the Au+Au reaction at 80 A MeV. Upper part: 4 snapshots of the density distribution in the reaction plane at 80, 150, 200 and 400 fm/c. Middle part: superposition of 100 of such events; open symbols: positions of IMFs in the reaction plane at 400 fm/c, filled symbols: positions of the 2 heaviest fragments. Bottom part: same as above but in the velocity space. Results for impact parameters 10 fm and 6 fm are given on the left and right side, respectively.

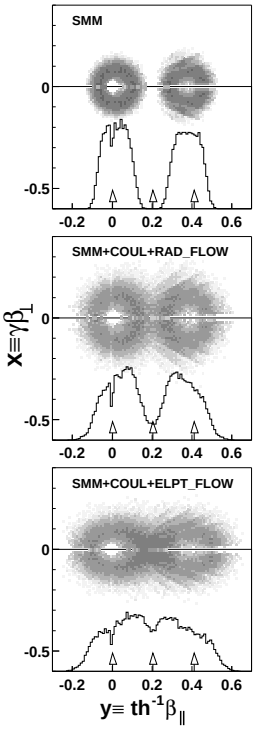

FIGURE 4. SMM predictions of the invariant cross sections of lithium ions emitted in the Au+Au reaction at 80 A MeV. Upper panel: original SMM. Middle panel: SMM with Coulomb interaction of the heavy partner included and isotropic radial flow of 1.5 MeV/nucleon. Bottom panel: same as middle, but elliptic flow was assumed instead of isotropic one.

Intuitively, one expects that midrapidity emissions are best described with microscopic dynamical models which

allow to study the temporal evolution of the system and incorporate the main ingredients of the nucleon-nucleon interactions. It has already been shown (see e.g. [3], [4], [7]), that some of them provide quite reasonable results as far as midrapidity emissions are concerned. In Fig. 3 we present some predictions of the molecular dynamics code CHIMERA [8]. The upper part of the figure presents 4 snapshots of the density distribution in the reaction plane of the Au+Au reaction at 80 A MeV at 80, 150, 200 and 400 fm/c. Below, a superposition of 100 of such events is presented, with the open symbols representing the positions of IMFs in the reaction plane at 400 fm/c, and with the filled symbols representing the positions of the heaviest fragments. At the bottom, the symbols represent the corresponding positions in the velocity space. Left part of the figure shows the events at 10 fm impact parameter and the right part for 6 fm, respectively.

The following conclusions might be drawn from the CHIMERA predictions: i) IMFs produced in the early phase of the reaction in peripheral collisions are emitted preferentially in–between the 2 heaviest fragments (or at midrapidity, when looking in velocity space); more violent collisions (see b=6 fm column) lead to: ii) strong deformation of the primary fragments which may persist for a long time scale, and to iii) multi–fragment emission and/or fission of primary fragments; iv) the shape of the emission pattern in the reaction plane might possibly suggest a scenario of emission from a rotating "hot spot" or from a rotating deformed source (see right part of Fig. 3).

Statistical multifragmentation models like SMM [9] or MMMC [10] in their standard versions can not account for midrapidity emissions. The predicted emission pattern is isotropic or forward–backward symmetric in the source frame. This can be viewed from the top panel of Fig. 4, which presents invariant cross sections of lithium fragments emitted in the Au+Au reaction at 80 A MeV. The midrapidity region remains unpopulated. The primary gold fragments were assumed to be excited to 3 MeV/nucleon, which corresponds to moderately peripheral collisions. This symmetry can be broken by inclusion of the Coulomb field of the heavy partner acting on the (multi)fragmenting excited nucleus [11]. The resulting asymmetric partitions with the heaviest fragments pushed apart and lighter fragments in–between turn out to be energetically preferred. The midrapidity region can be filled (see middle panel of Fig. 4, where additional radial flow of 1.5 MeV/nucleon has been added). Inclusion of an asymmetric flow pattern in longitudinal and transverse directions can further enhance the midrapidity component (see bottom panel of Fig. 4 which might be compared with the left panel of Fig. 2). Angular momentum as well as deformation effects may also be important.

The above figures show that, at least qualitatively, both, dynamical and statistical models can account for midrapidity emissions. The remaining question is how much of them originate from the statistical decay of the residue. It seems that at least a fraction of these emissions, in the vicinity of the Coulomb rings, can be interpreted in the framework of statistical models provided the Coulomb influence of the heavy partner is taken into account. This means that anisotropy does not necessarily imply non equilibrium. The definition of the equilibrated sources in peripheral symmetric heavy ion collisions may still be a non–trivial task.

TRANSVERSE VELOCITY DISTRIBUTIONS

As a potentially useful observable for further investigations we present in Fig. 5 the invariant transverse fragment velocity spectra for selected rapidity and centrality bins and as a function of the incident energy. These spectra are expected to be Gaussian for a thermally emitting source and, if Coulomb forces act in addition, peaked at the velocity corresponding to the Coulomb energy.

These features can be noticed in the left panel of Fig. 5. The transverse velocities of Li ions at projectile rapidities clearly show the Coulomb component. The peak at $\beta \approx 0.08$, corresponds to a Coulomb energy of 20 MeV expected on the basis of the fission systematics. It is the same for all bombarding energies, indicating emission from the surface of the heavy residues.

The Coulomb component is nearly absent or possibly spread out over a wide velocity range in the emissions at midrapidity where we observe two different scaling behaviors in the peripheral and central impact-parameter bins. In the central case (right panel of Fig. 5), the shapes are approximately Gaussian with an extra shoulder superimposed at lower incident energy, possibly due to Coulomb repulsion, and a width that *increases* considerably with increasing bombarding energy and with the fragment mass. This reflects the increasing importance of flow for central collisions with the increasing incident energy (see also [12]).

For peripheral reactions (middle panel), a particularly intriguing behavior is observed. The shapes of the spectra are between Gaussian and exponential and *invariant* with respect to the incident energy. The corresponding mean kinetic energies of about 40 MeV for lithium ions seem too large for a purely thermal origin and are larger than the value of 25 MeV obtained from the Goldhaber model [13] (with $p_F = 265$ MeV/c) but may reflect the additional Coulomb potential that is generated by the two residues in the neck region.

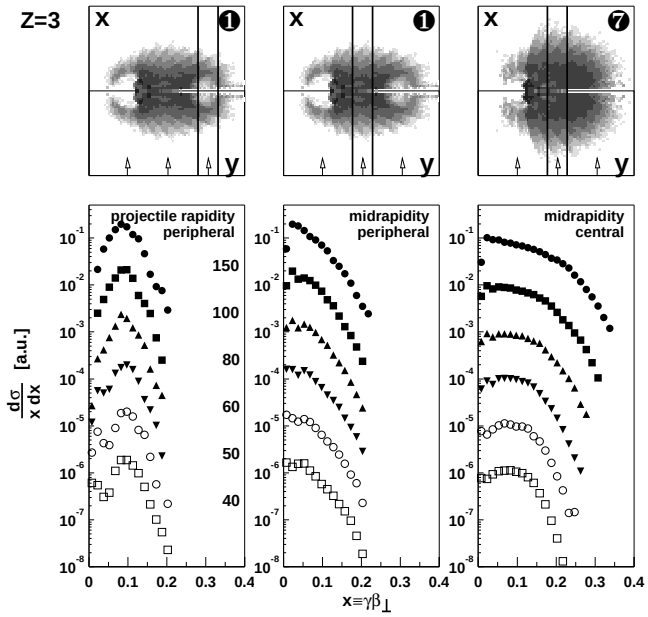

FIGURE 5. Invariant transverse velocity distributions for lithium ions at six bombarding energies specified in the left panel: from 40 (open squares at the bottom) to 150 A MeV (filled circles at the top) and for three selections in rapidity and centrality: projectile rapidity and peripheral (bin ❶) collisions (left panel), midrapidity and peripheral (bin ❶) collisions (middle panel) and midrapidity and central (bin ❼) collisions (right panel), respectively. The upper part of the figure presents the corresponding invariant plots with the indicated rapidity cuts.

Simulations of nucleon-nucleon collisions imply that the Pauli blocking of the collisions can be partly responsible for this invariance. The mean transverse energies of nucleons scattered into the midrapidity region show a very weak dependence on incident energy provided Pauli blocking is effective. Otherwise, mean transverse energies increase with the incident energy. Within a coalescence picture one might expect invariance of mean transverse energies at midrapidity also for fragments.

SUMMARY

The presented analysis was performed as a function of incident energy and of impact parameter, defined through the total transverse energy of light charged particles (Etrans12). For a given system, Etrans12 was found to scale linearly with the available energy up to a limit that, for the symmetric Au+Au and Xe+Sn systems, is at bombarding energies above 150 A MeV. Deviations from linear scaling above this limit were partly attributed to the anisotropy of the nucleon-nucleon cross section.

It was shown, on a qualitative level, that it is possible to attribute at least a fraction of midrapidity emissions to the thermal source. Clear separation of the equilibrated and the dynamical components requires further studies, including a consistent statistical treatment and a careful adjustment of flow, and possibly inclusion of angular momentum and deformation effects in statistical models. Dynamical models in turn, should be traced more carefully in terms of emission and equilibration times.

Transverse velocities at midrapidity for peripheral collisions were found to show a surprisingly weak dependence on incident energy. Simulations of nucleon–nucleon collisions imply that Pauli blocking of the collisions could be partly responsible for this invariance. On the contrary, transverse velocities at midrapidity for central collisions showed a strong dependence on incident energy reflecting the increasing importance of collective flow with increasing bombarding energy.

REFERENCES

1. J.F. Dempsey *et al.*, Phys. Rev. C **54**, 1710 (1996).
2. Y. Larochelle *et al.*, Phys. Rev. C **55**, 1869 (1997).
3. J. Łukasik *et al.*, Phys. Rev. C **55**, 1906 (1997).
4. E. Plagnol *et al.* Phys. Rev. C **61**, 014606 (2000).
5. J. Pouthas *et al.*, Nucl. Instr. Meth. in Phys. Res. **A357**, 418 (1995).
6. C. Cavata *et al.*, Phys. Rev. C **42**, 1760 (1990).
7. Ph. Eudes *et al.*, Phys. Rev. C **56**, 2003 (1997).
8. J. Łukasik and Z. Majka Acta Phys. Pol. B **24**, 1959 (1993).
9. J.P. Bondorf *et al.*, Phys. Rep. **257**, 133 (1995).
10. D.H.E. Gross, Rep. Prog. Phys. **53**, 605 (1990).
11. A.S. Botvina and I.N. Mishustin, Phys. Rev. C **63**, 061601(R) (2001).
12. F. Lavaud, E. Plagnol *et al.*, these proceedings.
13. A.S. Goldhaber Phys. Lett. **53B**, 306 (1974).